ELSEVIER

available at www.sciencedirect.com

ScienceDirect

journal homepage: www.elsevier.com/locate/jmatprotec

Author Index of Volume 207

Abdul Majeed, M., 321
Adiguzel, H.I., 258
Ahmed, K.S., 330
Aksan, M.A., 258
Angappan, S., 301
Ariffin, A.K., 118
Arifin Ahmad, Z., 235
Arun, K.V., 336
Augustin, C.O., 301

Balasivanandha Prabu, S., 53
Balasubramaniam, K., 315
Banerjee, S., 240
Birol, Y., 200
Brabazon, D., 307

Casalino, G., 63
Chakraborty, S.P., 240
Chan, C.Y., 72
Chang, H., 193
Chang, Y.-C., 193
Chen, W., 204
Chengyong, W., 154
Cheong, S.-K., 21
Chiang, K.-T., 89
Chow, H.-M., 180
Cui, W., 125

de Castro, P.M.S.T., 283
de Oliveira, F.M.F., 283

Fan, C.Z., 107

Geisinger, K.L., 315
Ghorbel, E., 63
Głownia, J., 147
Grover, A.K., 240
Gür, C.H., 211

Han, Z., 30
Hao, W., 172
Hashmi, M.S.J., 307
He, A., 130
Hong, L.C., 235
Hongtao, Z., 172
Horng, J.-T., 89
Houming, Z., 154
Hu, S.J., 204

Issa, A., 307

Jia, Y.Z., 107
Jiang, Y.H., 107
Jianguo, Y., 172
Jin, Y.-l., 265
John Berchmans, L., 301
Juster, N.P., 222

Kacar, I., 1
Kalandyk, B., 147
Kannan, E., 315
Karunamoorthy, L., 53, 343
Kawamura, Y., 112
Ke, G., 125
Kim, J., 112
Krishnamoorthy, R., 321

Labeas, G.N., 248
Lee, H.F., 72
Lee, J.-H., 21
Lee, S.-H., 21
Lee, S.-M., 180
Li, C., 187
Li, G.-j., 187
Li, J., 265
Li, J.M., 163
Lin, G.S., 204
Liu, C., 163
Lladó, J., 13

Ma, Z., 107
Malhotra, S.K., 321
Mauvoisin, G., 98
Md Akil, H., 235
Moreira, P.M.G.P., 283
Muhamad Nor, M.A.A., 235

Nayebi, A., 98
Noguchi, H., 21
Nor, S.S.M., 118

Ozturk, F., 1

Padmanabhan, K.A., 293
Pang, M., 271
Patirupanusara, P., 40
Peng, J., 163
Peng, Q., 187
Prasad, V.S.K., 315

Qianjian, G., 172

Raghunathan, S., 222
Rahman, M.M., 118
Ramakrishnan, R., 343
Ramamoorthy, B., 350
Ran, G., 46
Rubkumintara, T., 40

Şimşir, C., 211
Sánchez, B., 13
Sankaran, S., 293
Sankaran, S.P., 356
Selvi, S., 356
Shahida, B., 118
Shan, S.F., 107
Sharma, I.G., 240
Shen, B.-l., 187
Shen, X., 125
Shi, Y., 30
Sindhu, R., 301
Singh, K., 240
Srivatsavan, R., 356
Suri, A.K., 240
Suwanprateeb, J., 40
Suwanpreuk, W., 40

Tan, X., 222
Tang, C.S., 72
Tarlochan, F., 118
Toros, S., 1

Vaghefpour, H., 98
Venkatesha, C.S., 336
Vijayaraghavan, L., 321
Vijayarangan, S., 330

Wang, H.-H., 271
Wang, J., 187, 222
Wang, Q.G., 46
Wang, W.K., 107
Wang, X., 130
Wang, Y., 187

Xiushan, W., 172
Xu, K.-W., 276
Xu, W., 125

Yakinci, M.E., 258
Yan, X.-T., 222
Yang, H., 265, 276
Yang, L.-D., 180
Yang, Q., 130
Yeldose, B.C., 350
Yu, G., 271
Yu, W., 125

Zhang, L., 276
Zhang, L.Y., 107
Zhang, X.-g., 265
Zheng, C.-Y., 271
Zhenyu, Z., 154
Zhou, J.E., 46

Elsevier B.V.
doi:10.1016/S0924-0136(08)00645-6

JOURNAL OF MATERIALS PROCESSING TECHNOLOGY 207 (2008) 364–369

available at www.sciencedirect.com

ScienceDirect

journal homepage: www.elsevier.com/locate/jmatprotec

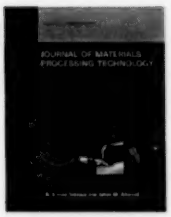

Subject Index of Volume 207

ABAQUS
Calculation of thermal stress affecting strip flatness change during run-out table cooling in hot steel strip rolling, 130
Al_2O_3 nanofluid
Fabrication of Al_2O_3 nanofluid by a plasma arc nanoparticles synthesis system, 193
Aluminium
Development of a local three-dimensional numerical simulation model for the laser forming process of aluminium components, 248
Aluminium alloys
Effect of cooling rate on solidified microstructure and mechanical properties of aluminium-A356 alloy, 107
Cooling slope casting and thixoforming of hypereutectic A390 alloy, 200
Aluminum–magnesium (Al–Mg) alloys
Review of warm forming of aluminum–magnesium alloys, 1
Artificial neural networks
Thermal error optimization modeling and real-time compensation on a CNC turning center, 172

Bending
Development of a local three-dimensional numerical simulation model for the laser forming process of aluminium components, 248
Biomaterial
Effect of fabrication processes on orientation growth of La/HAP crystal, 276
Buffer rod
Viscosity measurements of melts at high temperatures using ultrasonic guided waves, 315
Bulk metallic glasses
Electron beam welding of Zr-based BMG/Ni joints: Effect of beam irradiation position on mechanical and microstructural properties, 112
Burnishing operation
An investigation into the high performance of TiN-coated rollers in burnishing process, 350

Carbonitride precipitation
Effect of precipitation strengthening in low alloyed Mn–Ni cast steels, 147
Cast A356-T6 aluminum alloy
Precipitates and tensile fracture mechanism in a sand cast A356 aluminum alloy, 46
Ceramic foam
Preparation and characterization of ceramic foam produced via polymeric foam replication method, 235
Ceramic tool
A grey and fuzzy algorithms integrated approach to the optimization of turning Hadfield steel with Al_2O_3/TiC mixed ceramic tool, 89
Characterization
Studies on the development of protective coating on TZM alloy and its subsequent characterization, 240
Clamping pin
A comparison study on the effectiveness of stepped binder and weld line clamping pins on formability improvement for tailor-welded blanks, 204
CO_2 laser
3D transient thermal modelling of laser microchannel fabrication in lime-soda glass, 307
Coating
Studies on the development of protective coating on TZM alloy and its subsequent characterization, 240
Compaction
The effect of lubrication in reducing net friction in warm powder compaction process, 118
Composites
A.E. monitoring of ultrasonic machining of Al_2O_3/$LaPO_4$ composites, 321
Conductivity
Effect of antimony substitution on structural and electrical properties of $LaFeO_3$, 301
Contact stresses
Dynamic friction model and its application in flat rolling, 222
Cooling slope
Cooling slope casting and thixoforming of hypereutectic A390 alloy, 200
Co-precipitation
Effect of antimony substitution on structural and electrical properties of $LaFeO_3$, 301
Corona discharge
Effects of corona discharge treatment on the surface properties of wool fabrics, 125
Cracks
Microstructure study of laser welding cast nickel-based superalloy K418, 271
Crystal orientation
Effect of fabrication processes on orientation growth of La/HAP crystal, 276
CVN impact testing
Experimental investigations on fracture toughness and transition temperature in hard chrome coated structural materials, 336

Elsevier B.V.
doi:10.1016/S0924-0136(08)00646-8

Damage prediction
Microstructure-based finite element analysis of failure prediction in particle-reinforced metal–matrix composite, 53
Dendrite arm spacing
Effect of cooling rate on solidified microstructure and mechanical properties of aluminium-A356 alloy, 107
Drilling
Modeling of twist drills wear by a temperature-dependent friction law, 98
Dynamic characteristics
Dynamic characteristics of conjunction of lengthened shrink-fit holder and cutting tool in high-speed milling, 154

Electrical properties
A study on the thermoelectric power and thermal conductivity properties of the $Y_{1-x}Nd_xBa_2Cu_3O_{7-\delta}$ system, 258
Embedded passives
Embedding capacitors and resistors into printed circuit boards using a sequential lamination technique, 72

Fast cooling
Effect of cooling rate on solidified microstructure and mechanical properties of aluminium-A356 alloy, 107
Fatigue life
Fatigue behaviour of notched specimens of friction stir welded aluminium alloy 6063-T6, 283
Ferrite–bainite–martensite
Fatigue behavior of a multiphase medium carbon V-bearing microalloyed steel processed through two thermomechanical routes, 293
Ferritic stainless steel
Comparative study of hardfacing of valve seat ring using MMAW process, 356
Finite Element
Development of a local three-dimensional numerical simulation model for the laser forming process of aluminium components, 248
Finite element method
3D FEM simulation of steel quenching and investigation of the effect of asymmetric geometry on residual stress distribution, 211
Flatness
Calculation of thermal stress affecting strip flatness change during run-out table cooling in hot steel strip rolling, 130
Flexural strength
Tensile, flexural and interlaminar shear properties of woven jute and jute-glass fabric reinforced polyester composites, 330
Flow behavior
Effect of hot embossing process parameters on polymer flow and microchannel accuracy produced without vacuum, 163
Forging
Fatigue behavior of a multiphase medium carbon V-bearing microalloyed steel processed through two thermomechanical routes, 293
Formability
A comparison study on the effectiveness of stepped binder and weld line clamping pins on formability improvement for tailor-welded blanks, 204
Fracture mechanism
Precipitates and tensile fracture mechanism in a sand cast A356 aluminum alloy, 46
Fracture toughness
Effect of weld thermal cycle on microstructure and fracture toughness of simulated heat-affected zone for a 800 MPa grade high strength low alloy steel, 30
Experimental investigations on fracture toughness and transition temperature in hard chrome coated structural materials, 336
Friction
Modeling of twist drills wear by a temperature-dependent friction law, 98
Friction angle
Machining characteristic study of friction drilling on AISI 304 stainless steel, 180
Friction contact area ratio
Machining characteristic study of friction drilling on AISI 304 stainless steel, 180
Friction model
Dynamic friction model and its application in flat rolling, 222
Friction stir welding
Fatigue behaviour of notched specimens of friction stir welded aluminium alloy 6063-T6, 283
FRP laminated composites
A toughening and strengthening technique of hybrid composites with non-woven tissue, 21
Fuel calorific value
Fabrication of Al_2O_3 nanofluid by a plasma arc nanoparticles synthesis system, 193
Fuzzy
A grey and fuzzy algorithms integrated approach to the optimization of turning Hadfield steel with Al_2O_3/TiC mixed ceramic tool, 89

Gate design
Surface quality of PVC fittings based on the design of the sprue, 13
Genetic algorithm
Thermal error optimization modeling and real-time compensation on a CNC turning center, 172
Glass
3D transient thermal modelling of laser microchannel fabrication in lime-soda glass, 307
Viscosity measurements of melts at high temperatures using ultrasonic guided waves, 315
Grey relational analysis
A grey and fuzzy algorithms integrated approach to the optimization of turning Hadfield steel with Al_2O_3/TiC mixed ceramic tool, 89

Hadfield steel
A grey and fuzzy algorithms integrated approach to the optimization of turning Hadfield steel with Al_2O_3/TiC mixed ceramic tool, 89
Hand lay-up
Tensile, flexural and interlaminar shear properties of woven jute and jute-glass fabric reinforced polyester composites, 330
Hardfacing
Comparative study of hardfacing of valve seat ring using MMAW process, 356
Heat-affected zone (HAZ)
Effect of weld thermal cycle on microstructure and fracture toughness of simulated heat-affected zone for a 800 MPa grade high strength low alloy steel, 30
Comparative study of hardfacing of valve seat ring using MMAW process, 356

High replication accuracy
Effect of hot embossing process parameters on polymer flow and microchannel accuracy produced without vacuum, 163
High strength
Effect of precipitation strengthening in low alloyed Mn–Ni cast steels, 147
High-speed milling
Dynamic characteristics of conjunction of lengthened shrink-fit holder and cutting tool in high-speed milling, 154
Hollow tool
A.E. monitoring of ultrasonic machining of $Al_2O_3/LaPO_4$ composites, 321
Hot embossing
Effect of hot embossing process parameters on polymer flow and microchannel accuracy produced without vacuum, 163
Hot rolled strip
Calculation of thermal stress affecting strip flatness change during run-out table cooling in hot steel strip rolling, 130
HSLA steel
Effect of weld thermal cycle on microstructure and fracture toughness of simulated heat-affected zone for a 800 MPa grade high strength low alloy steel, 30
Hybrid concept
A toughening and strengthening technique of hybrid composites with non-woven tissue, 21
Hybrid prepreg
A toughening and strengthening technique of hybrid composites with non-woven tissue, 21
Hydroxyapatite
Effect of fabrication processes on orientation growth of La/HAP crystal, 276

ILSS
Tensile, flexural and interlaminar shear properties of woven jute and jute-glass fabric reinforced polyester composites, 330
Injection
Surface quality of PVC fittings based on the design of the sprue, 13
Interface
Electron beam welding of Zr-based BMG/Ni joints: Effect of beam irradiation position on mechanical and microstructural properties, 112

Jute-glass hybrid
Tensile, flexural and interlaminar shear properties of woven jute and jute-glass fabric reinforced polyester composites, 330

Lanthanum
Effect of fabrication processes on orientation growth of La/HAP crystal, 276
Laser beam forming
Development of a local three-dimensional numerical simulation model for the laser forming process of aluminium components, 248
Laser welding
Numerical model of CO_2 laser welding of thermoplastic polymers, 63
Lengthened shrink-fit holder
Dynamic characteristics of conjunction of lengthened shrink-fit holder and cutting tool in high-speed milling, 154
Lithium ion battery
Synthesis of LiV_3O_8 nanocrystallites as cathode materials for lithium ion batteries, 265
LiV_3O_8
Synthesis of LiV_3O_8 nanocrystallites as cathode materials for lithium ion batteries, 265
Local three-dimensional model
Development of a local three-dimensional numerical simulation model for the laser forming process of aluminium components, 248
Low cycle fatigue
Fatigue behavior of a multiphase medium carbon V-bearing microalloyed steel processed through two thermomechanical routes, 293
Low heating solid-state method
Synthesis of LiV_3O_8 nanocrystallites as cathode materials for lithium ion batteries, 265
Lubricant
The effect of lubrication in reducing net friction in warm powder compaction process, 118

Machining
A.E. monitoring of ultrasonic machining of $Al_2O_3/LaPO_4$ composites, 321
Martensitic stainless steel
Comparative study of hardfacing of valve seat ring using MMAW process, 356
Mechanical properties
Effect of binder content on the material properties of polymethyl methacrylate fabricated by three dimensional printing technique, 40
Medical applications
Effect of binder content on the material properties of polymethyl methacrylate fabricated by three dimensional printing technique, 40
Metal forming
Dynamic friction model and its application in flat rolling, 222
Metal powder
The effect of lubrication in reducing net friction in warm powder compaction process, 118
Metal–matrix composite
Microstructure-based finite element analysis of failure prediction in particle-reinforced metal–matrix composite, 53
Microalloyed cast steels
Effect of precipitation strengthening in low alloyed Mn–Ni cast steels, 147
Microchannels
3D transient thermal modelling of laser microchannel fabrication in lime-soda glass, 307
Microhardness
Effect of cooling rate on solidified microstructure and mechanical properties of aluminium-A356 alloy, 107
Microstructures
Precipitates and tensile fracture mechanism in a sand cast A356 aluminum alloy, 46
Influence of salt bath nitrocarburizing and post-oxidation process on surface microstructure evolution of 17-4PH stainless steel, 187
Fatigue behaviour of notched specimens of friction stir welded aluminium alloy 6063-T6, 283
Microstructure-based finite element analysis
Microstructure-based finite element analysis of failure prediction in particle-reinforced metal–matrix composite, 53

Mixing time
The effect of lubrication in reducing net friction in warm powder compaction process, 118
MMAW process
Comparative study of hardfacing of valve seat ring using MMAW process, 356
Modal parameter
Dynamic characteristics of conjunction of lengthened shrink-fit holder and cutting tool in high-speed milling, 154
MRR
Modeling and multi-response optimization of Inconel 718 on machining of CNC WEDM process, 343
MRSN
Modeling and multi-response optimization of Inconel 718 on machining of CNC WEDM process, 343

Nanocrystallite
Synthesis of LiV_3O_8 nanocrystallites as cathode materials for lithium ion batteries, 265
Nanomaterial
Effect of fabrication processes on orientation growth of La/HAP crystal, 276
NC machine tool
Thermal error optimization modeling and real-time compensation on a CNC turning center, 172
Needle carbides
Microstructure study of laser welding cast nickel-based superalloy K418, 271
Ni metal
Electron beam welding of Zr-based BMG/Ni joints: Effect of beam irradiation position on mechanical and microstructural properties, 112
Nickel-based superalloy
Microstructure study of laser welding cast nickel-based superalloy K418, 271
No-chip drilling
Machining characteristic study of friction drilling on AISI 304 stainless steel, 180
Non-woven tissue prepreg
A toughening and strengthening technique of hybrid composites with non-woven tissue, 21
Numerical model
Numerical model of CO_2 laser welding of thermoplastic polymers, 63

Optimization
A grey and fuzzy algorithms integrated approach to the optimization of turning Hadfield steel with Al_2O_3/TiC mixed ceramic tool, 89
Optimization modeling
Thermal error optimization modeling and real-time compensation on a CNC turning center, 172
Oxidation
Studies on the development of protective coating on TZM alloy and its subsequent characterization, 240

Pack cementation
Studies on the development of protective coating on TZM alloy and its subsequent characterization, 240
Perovskites
Effect of antimony substitution on structural and electrical properties of $LaFeO_3$, 301
PFZ
Precipitates and tensile fracture mechanism in a sand cast A356 aluminum alloy, 46
Phase transformation
3D FEM simulation of steel quenching and investigation of the effect of asymmetric geometry on residual stress distribution, 211
Pin-on-disc apparatus
Comparative study of hardfacing of valve seat ring using MMAW process, 356
Plasma arc
Fabrication of Al_2O_3 nanofluid by a plasma arc nanoparticles synthesis system, 193
Plasticity
Dynamic friction model and its application in flat rolling, 222
Polymeric foam replication method
Preparation and characterization of ceramic foam produced via polymeric foam replication method, 235
Polymethyl methacrylate
Effect of binder content on the material properties of polymethyl methacrylate fabricated by three dimensional printing technique, 40
Process conditions
Effect of hot embossing process parameters on polymer flow and microchannel accuracy produced without vacuum, 163
Production technique
A toughening and strengthening technique of hybrid composites with non-woven tissue, 21
PVC
Surface quality of PVC fittings based on the design of the sprue, 13

QPQ salt bath
Influence of salt bath nitrocarburizing and post-oxidation process on surface microstructure evolution of 17-4PH stainless steel, 187
Quenching
3D FEM simulation of steel quenching and investigation of the effect of asymmetric geometry on residual stress distribution, 211

Reactive sputtering
An investigation into the high performance of TiN-coated rollers in burnishing process, 350
Reflection factor
Viscosity measurements of melts at high temperatures using ultrasonic guided waves, 315
Residual stress
3D FEM simulation of steel quenching and investigation of the effect of asymmetric geometry on residual stress distribution, 211
Rolling
Dynamic friction model and its application in flat rolling, 222
Fatigue behavior of a multiphase medium carbon V-bearing microalloyed steel processed through two thermomechanical routes, 293
Run-out table
Calculation of thermal stress affecting strip flatness change during run-out table cooling in hot steel strip rolling, 130

5XXX series
Review of warm forming of aluminum–magnesium alloys, 1
17-4PH stainless steel
Influence of salt bath nitrocarburizing and post-oxidation process on surface microstructure evolution of 17-4PH stainless steel, 187

Scanning electron microscopy
Fatigue behaviour of notched specimens of friction stir welded aluminium alloy 6063-T6, 283
SEM
Influence of salt bath nitrocarburizing and post-oxidation process on surface microstructure evolution of 17-4PH stainless steel, 187
SEM fractography
Experimental investigations on fracture toughness and transition temperature in hard chrome coated structural materials, 336
Sequential lamination
Embedding capacitors and resistors into printed circuit boards using a sequential lamination technique, 72
Simulation
3D FEM simulation of steel quenching and investigation of the effect of asymmetric geometry on residual stress distribution, 211
Solid freeform fabrication
Effect of binder content on the material properties of polymethyl methacrylate fabricated by three dimensional printing technique, 40
Solid tool
A.E. monitoring of ultrasonic machining of $Al_2O_3/LaPO_4$ composites, 321
Steel
3D FEM simulation of steel quenching and investigation of the effect of asymmetric geometry on residual stress distribution, 211
Stepped binder
A comparison study on the effectiveness of stepped binder and weld line clamping pins on formability improvement for tailor-welded blanks, 204
Strain-based approach of fatigue life
Fatigue behaviour of notched specimens of friction stir welded aluminium alloy 6063-T6, 283
Strength
Effect of cooling rate on solidified microstructure and mechanical properties of aluminium-A356 alloy, 107
Superconductors
A study on the thermoelectric power and thermal conductivity properties of the $Y_{1-x}Nd_xBa_2Cu_3O_{7-\delta}$ system, 258
Surface characteristics
An investigation into the high performance of TiN-coated rollers in burnishing process, 350
Surface properties
Effects of corona discharge treatment on the surface properties of wool fabrics, 125
Surface quality
Surface quality of PVC fittings based on the design of the sprue, 13
Surface roughness
Machining characteristic study of friction drilling on AISI 304 stainless steel, 180
Modeling and multi-response optimization of Inconel 718 on machining of CNC WEDM process, 343

Taguchi method
Machining characteristic study of friction drilling on AISI 304 stainless steel, 180
Temperature
Modeling of twist drills wear by a temperature-dependent friction law, 98
Tensile properties
Precipitates and tensile fracture mechanism in a sand cast A356 aluminum alloy, 46
Thermal conductivity
A study on the thermoelectric power and thermal conductivity properties of the $Y_{1-x}Nd_xBa_2Cu_3O_{7-\delta}$ system, 258
Thermal error
Thermal error optimization modeling and real-time compensation on a CNC turning center, 172
Thermal friction drilling
Machining characteristic study of friction drilling on AISI 304 stainless steel, 180
Thermal modelling
3D transient thermal modelling of laser microchannel fabrication in lime-soda glass, 307
Thermal stress
Calculation of thermal stress affecting strip flatness change during run-out table cooling in hot steel strip rolling, 130
Thermal–structural analysis
Development of a local three-dimensional numerical simulation model for the laser forming process of aluminium components, 248
Thermoplastic polymers
Numerical model of CO_2 laser welding of thermoplastic polymers, 63
Thermo-viscoplastic model
Modeling of twist drills wear by a temperature-dependent friction law, 98
Thin film process
Embedding capacitors and resistors into printed circuit boards using a sequential lamination technique, 72
Thixoforming
Cooling slope casting and thixoforming of hypereutectic A390 alloy, 200
Three dimensional printing
Effect of binder content on the material properties of polymethyl methacrylate fabricated by three dimensional printing technique, 40
Transition temperature
Experimental investigations on fracture toughness and transition temperature in hard chrome coated structural materials, 336
TWB
A comparison study on the effectiveness of stepped binder and weld line clamping pins on formability improvement for tailor-welded blanks, 204
TZM alloy
Studies on the development of protective coating on TZM alloy and its subsequent characterization, 240

Ultrasonic
A.E. monitoring of ultrasonic machining of $Al_2O_3/LaPO_4$ composites, 321
Ultrasonic guided wave
Viscosity measurements of melts at high temperatures using ultrasonic guided waves, 315
UV–Vis absorption
Fabrication of Al_2O_3 nanofluid by a plasma arc nanoparticles synthesis system, 193

Vanadium microaddition
Effect of precipitation strengthening in low alloyed Mn–Ni cast steels, 147
Viscosity
Viscosity measurements of melts at high temperatures using ultrasonic guided waves, 315

Warm forming
Review of warm forming of aluminum–magnesium alloys, 1
WEDM
Modeling and multi-response optimization of Inconel 718 on machining of CNC WEDM process, 343
Weight percent
The effect of lubrication in reducing net friction in warm powder compaction process, 118
Weld line movement
A comparison study on the effectiveness of stepped binder and weld line clamping pins on formability improvement for tailor-welded blanks, 204
Welded joint
Effect of weld thermal cycle on microstructure and fracture toughness of simulated heat-affected zone for a 800 MPa grade high strength low alloy steel, 30
Welding
Electron beam welding of Zr-based BMG/Ni joints: Effect of beam irradiation position on mechanical and microstructural properties, 112
Wool fabric
Effects of corona discharge treatment on the surface properties of wool fabrics, 125

XPS analysis
Effects of corona discharge treatment on the surface properties of wool fabrics, 125
X-ray diffraction
Influence of salt bath nitrocarburizing and post-oxidation process on surface microstructure evolution of 17-4PH stainless steel, 187
Effect of antimony substitution on structural and electrical properties of $LaFeO_3$, 301